

# Role of amino acid transporter LAT2 in the activation of mTORC1 pathway and the pathogenesis of crescentic glomerulonephritis

Ryota Kurayama<sup>1</sup>, Noriko Ito<sup>1</sup>, Yukino Nishibori<sup>1</sup>, Daisuke Fukuhara<sup>1</sup>, Yoshihiro Akimoto<sup>2</sup>, Eiji Higashihara<sup>3</sup>, Yasuhito Ishigaki<sup>4</sup>, Yoshimichi Sai<sup>5</sup>, Ken-ichi Miyamoto<sup>5</sup>, Hitoshi Endou<sup>6</sup>, Yoshikatstu Kanai<sup>7</sup> and Kunimasa Yan<sup>1</sup>

Molecular mechanisms and signaling pathways leading to cellular proliferation and lesion formation in the crescentic glomerulonephritis (CGN) remain elusive. In the present study we have explored a potential role of the mammalian target of rapamycin complex 1 (mTORC1) signaling pathway and amino acid transporter (LAT) in the pathogenesis of CGN. Immunohistochemistry and western blot analysis of glomeruli isolated from a rat model of CGN revealed that activation of mTORC1 preceded crescent formation in glomerular parietal epithelial cells (PECs) and podocytes. Daily treatment of rats with the mTOR inhibitor everolimus just after induction of CGN was not beneficial and instead led to increased cellular necrosis of PECs. However, daily treatment starting 7 days after the onset of CGN was beneficial and maintained intact glomeruli. Out of three forms of L-type neutral amino acid transporters (LAT1–LAT3) studied here, only LAT2 was found to be upregulated in the PECs and podocytes in advance of the crescent formation as well as in the crescent lesion itself. Cell culture study revealed that plasma membrane expression of LAT2 markedly stimulated mTORC1 signaling pathway, which was significantly abrogated by coexistence of LAT inhibitor. Finally, LAT inhibitor significantly abrogated development of crescent formation of CGN on day 7. Our data suggest that LAT2 may have a pivotal role in the pathogenesis of CGN by activating the mTORC1 pathway in the glomerular epithelial cells.

*Laboratory Investigation* (2011) 91, 992–1006; doi:10.1038/labinvest.2011.43; published online 14 March 2011

**KEYWORDS:** branched-chain amino acid; crescentic glomerulonephritis; everolimus; LAT; mTORC1

Crescentic glomerulonephritis (CGN) is the most severe form of glomerulonephritis, and if untreated, progresses to end-stage renal failure within days or weeks of diagnosis. Despite different etiologies and clinical manifestations among patients with CGN, there is a common glomerular pathology characterized by the disruption of glomerular basement membrane (GBM), followed by the flow of plasma proteins and inflammatory cells into the Bowman's space.<sup>1</sup> Several studies suggest that proliferating glomerular epithelial cells and accumulation of infiltrated macrophages are the main components of the cellular crescents.<sup>2–6</sup> Recent reports have further revealed that the cellular crescent lesions in CGN consist of podocytes in addition to glomerular parietal epithelial cells (PECs) and macrophages.<sup>7–9</sup> It is increasingly evident that proinflammatory cytokines and growth

hormones released by proliferating cells in the glomerulus are involved in the pathogenesis of crescent formation.<sup>10–13</sup> These factors stimulate the p38 mitogen-activated protein kinase (MAPK) pathway, resulting in the production of inflammatory mediators.<sup>14–16</sup> The involvement of the MAPK pathway in the pathogenesis of CGN was first reported by Bokemeyer *et al*,<sup>17</sup> who demonstrated a rapid and sustained activation of extracellular signal-regulated kinase in the glomeruli isolated from rat model of anti-GBM nephritis. A further study demonstrated that both podocytes and the crescent lesion are the main source of p38MAPK activation, although additional signaling pathways could not be excluded.<sup>18</sup>

Recent studies suggest that the mammalian target of rapamycin complex 1 (mTORC1) cascade has a regulatory

<sup>1</sup>Department of Pediatrics, Kyorin University School of Medicine, Tokyo, Japan; <sup>2</sup>Department of Anatomy, Kyorin University School of Medicine, Tokyo, Japan; <sup>3</sup>Department of Urology, Kyorin University School of Medicine, Tokyo, Japan; <sup>4</sup>Medical Research Institute, Kanazawa Medical University, Kanazawa, Japan; <sup>5</sup>Department of Hospital Pharmacy, Kanazawa University, Kanazawa, Japan; <sup>6</sup>Department of Toxicology and Pharmacology, Kyorin University School of Medicine, Tokyo, Japan; <sup>7</sup>Department of Pharmacology, Osaka University Graduate School of Medicine, Osaka, Japan  
Correspondence: Professor K Yan, MD, PhD, Department of Pediatrics, Kyorin University School of Medicine, 6-20-2 Shinkawa, Mitaka, Tokyo 181-8611, Japan.  
E-mail: kuniyan@ks.kyorin-u.ac.jp

Received 17 May 2010; revised 19 November 2010; accepted 9 January 2011

role in the signaling pathways that control cellular growth and proliferation.<sup>19,20</sup> Signaling through the mTORC1 pathway is activated by growth factors and nutrients, of which branched-chain amino acids (BCAA) are potent intracellular stimulators.<sup>21–24</sup> Active transport of amino acids across the plasma membrane is mediated by several types of amino acid transporters, among which the system L amino acid transporter (LAT) family preferentially selects BCAA as their substrates.<sup>25,26</sup> So far, four LATs (LAT1–LAT4) have been identified at the molecular level. LAT1<sup>27</sup> has been found in many malignant cells;<sup>28,29</sup> however, its clear expression in normal tissues has been only reported in the vascular endothelial cells forming the blood–brain barrier<sup>30,31</sup> and syncytiotrophoblastic cells of the placenta.<sup>32</sup> Expression of LAT2 has been shown in the epithelium of kidney proximal tubules and the digestive tract.<sup>33–37</sup> LAT3 and LAT4 have been localized to the apical plasma membrane of podocytes<sup>38</sup> and the distal tubules and collecting ducts,<sup>39</sup> respectively. In the present study, we have used a rat model of CGN to investigate the activation of mTORC1 pathway as a possible underlying factor in the crescent formation of glomerular epithelial cells. We show that the activation of mTORC1 pathway precedes the crescent formation in the glomeruli of rats with CGN and that the functional activity of LAT2 on the plasma membrane of cells stimulates mTORC1 signaling pathway.

## MATERIALS AND METHODS

### Antibodies and Reagents

Polyclonal antibodies against human LAT1 (JH5501), human LAT2 (JH6524), rat LAT2 (JH7057) and rat heavy chain of 4F2 antigen (4F2hc) (JH5502) were obtained from Trans Genic (Kumamoto, Japan). Anti-mouse LAT3 polyclonal antibody was previously described.<sup>38</sup> The following antibodies were purchased from the suppliers as indicated: anti-phospho-S6 ribosomal protein rabbit monoclonal (91B2) (Ser235/236), anti-p70S6 kinase rabbit polyclonal, anti-phospho-p70S6 kinase rabbit polyclonal (Thr389), anti-4E-BP1 rabbit polyclonal and anti-phospho-4E-BP1 rabbit polyclonal (Tyr37/46) (Cell Signaling Technology, Beverly, MA, USA); anti-vascular endothelial growth factor (VEGF) monoclonal (Novus Biologicals, Littleton, CO, USA); anti-AKT1 phospho-specific (pS473) polyclonal (Rockland, Gilbertsville, PA, USA); anti- $\beta$ -actin monoclonal (Sigma-Aldrich, St Louis, MO, USA); goat anti-mouse and goat anti-rabbit horseradish peroxidase (Dako, Kyoto, Japan) and Alexa Fluor 488-conjugated goat anti-rabbit IgG (Molecular Probes, Eugene, OR, USA). Nephritogenic anti-GBM monoclonal antibody (clone b35) was purchased from Chondrex (Redmond, Wash, USA).<sup>40</sup> Microemulsion formulations (self-microemulsifying drug delivery system) of mTOR inhibitor, everolimus, and vehicle, were kindly donated by Novartis Pharma AG (Basel, Switzerland). 2-Amino-2 norbornate-carboxylic acid (BCH), a specific

functional inhibitor of LAT1 and LAT2, was purchased from Sigma.

### Animal Experiments

All animal experiments were conducted according to the guidelines of the Laboratory Animals Center of Kyorin University School of Medicine. In the present study, a total of 67 female WKY/NCrj rats between 4 and 6 weeks old and weighing 100–180 g were purchased from Charles River Japan (Yokohama, Japan). We performed three animal experiments as indicated in Supplementary Table 1. Experiment 1 was conducted to determine the development of CGN and remove the kidney and isolate glomeruli. To do so, anti-GBM antibody or saline solution was intraperitoneally injected to 42 rats (Supplementary Table 1).<sup>40</sup> Animals were caged individually in metabolic cages for urine sample collection. Individual 24-h urine samples collected from each rat were used for urine analysis. The amounts of urinary protein excretion and creatinine were measured by albumin assay kit (Wako, Tokyo, Japan) and the Jaffe assay, respectively. Rats were anesthetized with Avertin pentobarbitone and their kidneys were removed and processed for immunohistochemistry. Pure glomeruli were isolated by subjecting the rats to magnetic beads perfusion method as previously described.<sup>38</sup> To isolate pure glomeruli with intact Bowman's capsule, collagenase treatment was excluded. Isolated glomeruli were used for western blot analysis and reverse transcriptase-polymerase chain reaction (RT-PCR).

Experiment 2 was conducted to evaluate the effect of mTORC1 inhibitor on the progress of CGN. A total of 18 rats were subjected to the intraperitoneal injection of anti-GBM antibody as described above. Rats were subjected to administration of everolimus via gavage at a dose of 2.5 mg/kg body weight per day or a vehicle solution as control. In the early treatment (Figure 1), everolimus and vehicle solutions were administered on day 0, just after injection of anti-GBM antibody, and continued daily through day 6. On day 7, rats were killed and their kidney was then subjected to immunohistochemistry and isolation of glomeruli. In the late treatment (Figure 1), everolimus and vehicle solution were started 7 days after injection of anti-GBM antibody and continued through day 13 and the animals were then killed on day 14.

Experiment 3 was conducted to evaluate the effect of LAT inhibitor on the progress of CGN. A total of seven rats were subjected to the injection of anti-GBM antibody. LAT-inhibitor BCH (200  $\mu$ M/100 g body weight per day)<sup>41</sup> or saline solution was intravenously injected into the rat tail vein from day 0 and continued through day 6. Animals were killed and their kidney was subjected to immunohistochemistry.

### Immunohistochemistry

Samples from rat kidney cortex were fixed in 4% paraformaldehyde for 2 h at 4°C, embedded in paraffin wax. The slides were subjected to autoclave heating at 120°C for

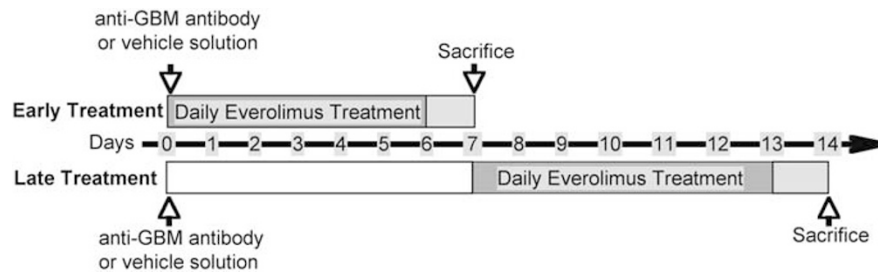


**Figure 1** Experimental overview of experiment 2 (Supplementary Table 1) showing the comparison between early and late treatments of everolimus.

10 min, incubated with 1% H<sub>2</sub>O<sub>2</sub>/phosphate-buffered saline (PBS) for 30 min, and then treated with blocking buffer (3% BSA, 5% goat serum and 0.05% Tween-20 in PBS) for 60 min. Thereafter, slides were reacted with primary antibodies: anti-LAT1 (2.0 µg/ml), anti-LAT2 (2.0 µg/ml), anti-LAT3 (3.0 µg/ml), anti-4F2hc (4.0 µg/ml), anti-AKT1 phospho-specific (pS473) (1:100) or anti-phospho-S6 ribosomal protein antibody (1:75), and incubated overnight at 4°C. After three washing steps with PBS, the slides were incubated with biotinylated secondary antibody and the immune complexes were detected by an avidin–biotin complex detection system (ABC KIT, Vector Laboratories, Burlingame, CA, USA).

### Renal Histology

Rat kidney sections were fixed with 4% paraformaldehyde and deparaffinized, stained with periodic acid-Schiff (PAS) and examined by light microscopy. Ratio of cellular crescents and fibrinoid necrosis was determined by counting between 250 and 300 glomeruli per animal. Data were expressed as the means ± s.e.m. Statistical significance of differences was calculated by the two-tailed Mann–Whitney *U*-test.

### Immunofluorescence and Confocal Microscopy

The cell line (S2) stably expressing human LAT2 (S2-hLAT2) was previously described.<sup>42</sup> Cells were cultured in RITC 80-7 medium (IWAKI, Tokyo, Japan) containing 5% FBS, 500 µg/ml G418, 10 mg/ml transferrin, 0.08 U/ml insulin and 10 ng/ml recombinant EGF in a 33°C incubator with an atmosphere of 5% CO<sub>2</sub>. Cells cultured on glass cover slips were fixed with 3% formaldehyde in PBS for 15 min at room temperature and reacted with anti-human LAT2 antibodies (1.0 µg/ml) for 60 min at room temperature. Immunocomplex was visualized by Alexa Fluor 488-conjugated goat anti-rabbit IgG and phalloidin. Cells were examined under a confocal laser scanning microscope equipped with a krypton/argon laser (model MRC1024; Bio-Rad, Hercules, CA, USA).

### Amino Acid Starvation Assay

S2-hLAT2 cells and wild-type S2 cells were cultured in standard medium (RITC 80-7 medium containing HEPES buffer and NaHCO<sub>3</sub> without growth factors and FBS) for 17 h. Thereafter, cells were starved in PBS solution containing

1% glucose for 120 min. For specific inhibition of LAT2, cells were cultured in standard medium in the absence or presence of 20 mM of BCH in a time-dependent manner for up to 120 min. Cells were finally collected and their lysates were subjected to western blot analysis as described below.

### Protein Extraction and Western Blot Analysis

Glomerular samples and cultured cells were lysed in ice-cold lysis buffer and isolation of total proteins was carried out as described.<sup>38</sup> Total protein content in each sample was measured by Bradford method. For western blot analysis, 50 µg of proteins were separated by SDS-PAGE using 4–20% gradient or 10% gels under reducing conditions. Proteins were transferred onto PVDF membranes by electroblotting and reacted with antibodies: anti-human and rat LAT2 (0.5 µg/ml, respectively), anti-rat 4F2hc (0.5 µg/ml), anti-phospho-S6 ribosomal protein (1:1000), anti-phospho-p70S6 kinase (1:1000), anti-p70S6 kinase, anti-phospho-4E-BP1 (1:1000), anti-4E-BP1 (1:1000), anti-VEGF (2 µg/ml); anti-AKT1 phospho-specific (1:1000) or anti-β-actin (1:1000). Protein bands were visualized by using HRP-conjugated secondary goat antibodies and a chemiluminescence kit (Life Science Products, Boston, MA, USA). Photosensitive films (BioMax XAR, Kodak, Rochester, NY, USA) were used to visualize protein bands. For semi-quantification of protein bands, films were scanned and band intensities were analyzed by the NIH Image software ver.1.63.

### RT-PCR

Total RNA was obtained from isolated glomeruli and the rest of kidney cortex. The RT-PCR for rat LAT2 was carried out using sense primer 5'-TCATTGGCTCCGGAATCTTC-3' and antisense primer 5'-ATGCATTCTTTGGCTCCAGC-3'. Rat 4F2hc was detected by using sense primer 5'-CATGGTTCCTCCCTCCTCAG-3' and antisense primer 5'-GGAGAAGAGGCCAGATGAGG-3'; and rat β-actin, by using sense primer 5'-GACAACGGCTCCGGCATGTGCA-3' and antisense primer 5'-ATGACCTGGCCGTCAGGCAGCT-3'. Total RNA (1 µg) was amplified under the following conditions: 25 cycles at 94°C for 1 min, 58°C for 1 min and 72°C for 2 min. The size of PCR products were analyzed by electrophoresis on 1% agarose gels and their sequences were confirmed by direct

sequencing of each PCR product after purification from agarose gels.

### Measurement of Everolimus Concentration

Trough level of everolimus concentration was determined by using ethylenediaminetetraacetic acid-anti-coagulated whole-blood samples that were collected from CGN rats on day 7 and control (vehicle) rats. Aliquots of whole blood were mixed with 2.5 vol. of protein precipitation reagent (methanol/acetonitrile 50%:50% (vol/vol) containing 100 ng/ml ascomycin, which was used as the internal standard), vortexed for 1 min and stored at  $-20^{\circ}\text{C}$  for at least 10 min. The tubes were again vortexed for 1 min and centrifuged at 20 000 g for 10 min, and the clear upper layer of supernatants were transferred into vials for liquid chromatography/mass spectrometry (LC-MS) consisted of a Shimadzu LCMS-2020 (Shimadzu, Tokyo, Japan) mass spectrometer and Prominence ultra-fast liquid chromatograph system (Shimadzu). The analytical column was a Shim-pack XR-ODS 75 mm  $\times$  2.0 mm column from Shimadzu. The mass spectrometer was operated in the positive and negative electrospray ionization mode. Full-scan spectra were acquired over the mass range of 700–1050 a.m.u., and sodium, potassium and ammonium adducts, as well as deprotonated form were confirmed for each analyte. Single-ion-monitoring mode was used for analyte quantitation by simultaneously monitoring quasi-molecular ions,  $m/z$  957 for [everolimus-H] $^{-}$ ,  $m/z$  913 for [rapamycin-H] $^{-}$  and  $m/z$  791 for [ascomycin-H] $^{-}$ . LCMS solution software (ver. 5) was used for acquisition of the LC-MS data, construction of the internal calibration curves and derivation of the regression equations.

## RESULTS

### Activation of mTORC1 Pathway in CGN

Experiment 1 was investigated to determine whether mTORC1 pathway is involved in the pathogenesis of CGN. Rats were injected with anti-GBM antibody or saline (control) and the development of CGN was assessed by blood and urine examination and renal pathology followed for 7 days. Following the injection of antibody, the rats developed significant proteinuria on day 2 followed by heavy proteinuria and macrohematuria on day 5 and day 7, respectively (Figure 2). Although no significant change of serum creatinine level between CGN rats and control rats was observed, CGN rats obviously showed the lower level of serum albumin compared with that of control rats (Supplementary Table 2). Two serial sections from the kidney cortex were subjected to immunohistochemistry for p-S6RP, an activated form of downstream protein of the mTORC1 cascade, and PAS staining, respectively. As depicted in Figure 3a, immunohistochemistry showed that p-S6RP could be detected even in the control glomeruli of some PECs (arrow) and podocytes (arrowhead). However, the intensity of p-S6RP was obviously increased especially in majority of PECs (arrow) 2 days after induction of glomerulonephritis, when no apparent cellular

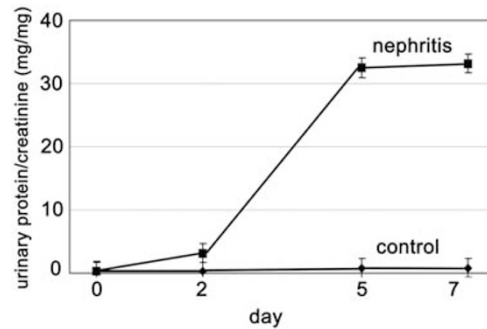


**Figure 2** Progression of proteinuria in crescentic glomerulonephritis (CGN). Rats were injected with either anti-glomerular basement membrane (GBM) antibody (nephritis,  $n = 6$ ) or saline solution (control,  $n = 6$ ). Proteinuria was presented as a ratio of urinary albumin and creatinine (mg/mg). Data are shown as mean  $\pm$  s.e.

crescent or hypertrophy of glomerular epithelial cells could be detected yet. Interestingly, in the glomeruli on days 5 and 7, drastically increased expression of p-S6RP was detected in the cellular crescent lesions (asterisk).

To further verify whether activation of mTORC1 pathway is indeed involved in the pathogenesis of CGN, we next examined the inhibitory effect of an mTORC1 inhibitor everolimus on the crescent formation. To do so, we induced glomerulonephritis in rats and studied the effect of both early and late treatment of everolimus (Figure 1). PAS staining revealed that rats receiving early treatment of everolimus had a lower ratio of cellular crescent lesions compared with the control group treated with vehicle solution (Figure 3b). However, the ratio of glomerular fibrinoid necrosis in the everolimus-treated rats was significantly higher than that of vehicle group, indicating that there was no significant difference in the everolimus and vehicle-treated rats with respect to the ratio of intact glomeruli without extracapillary lesions (Figure 3b). On the other hand, in the late treatment, in which rats were given everolimus, starting 7 days after the insult, it not only reduced cellular crescent formation in the glomeruli but also significantly rescued the number of intact glomeruli without extracapillary lesions (Figure 3b). To confirm the actual existence of everolimus in the rat body of the present study, its trough level in the whole blood from total six rats subjected to early experiment was measured as described in the Supplementary Methods. The concentration in the whole blood from everolimus-treated rats was  $22.9 \pm 3.2$  ng/ml (mean  $\pm$  s.e.,  $n = 3$ ), whereas that from vehicle-treated rats was not detectable ( $n = 3$ ), indicating that everolimus must have indeed exhibited its pharmacological action in the rat body. Moreover, immunohistochemistry showed that the intensity of p-S6RP in the cellular crescent lesion of CGN glomeruli was actually reduced by treatment with everolimus, suggesting that this drug might have directly effected on the diseased glomeruli (Figure 4a). To further verify the evidence of action of everolimus on the diseased glomeruli, we utilized western blot analysis of p-S6RP by



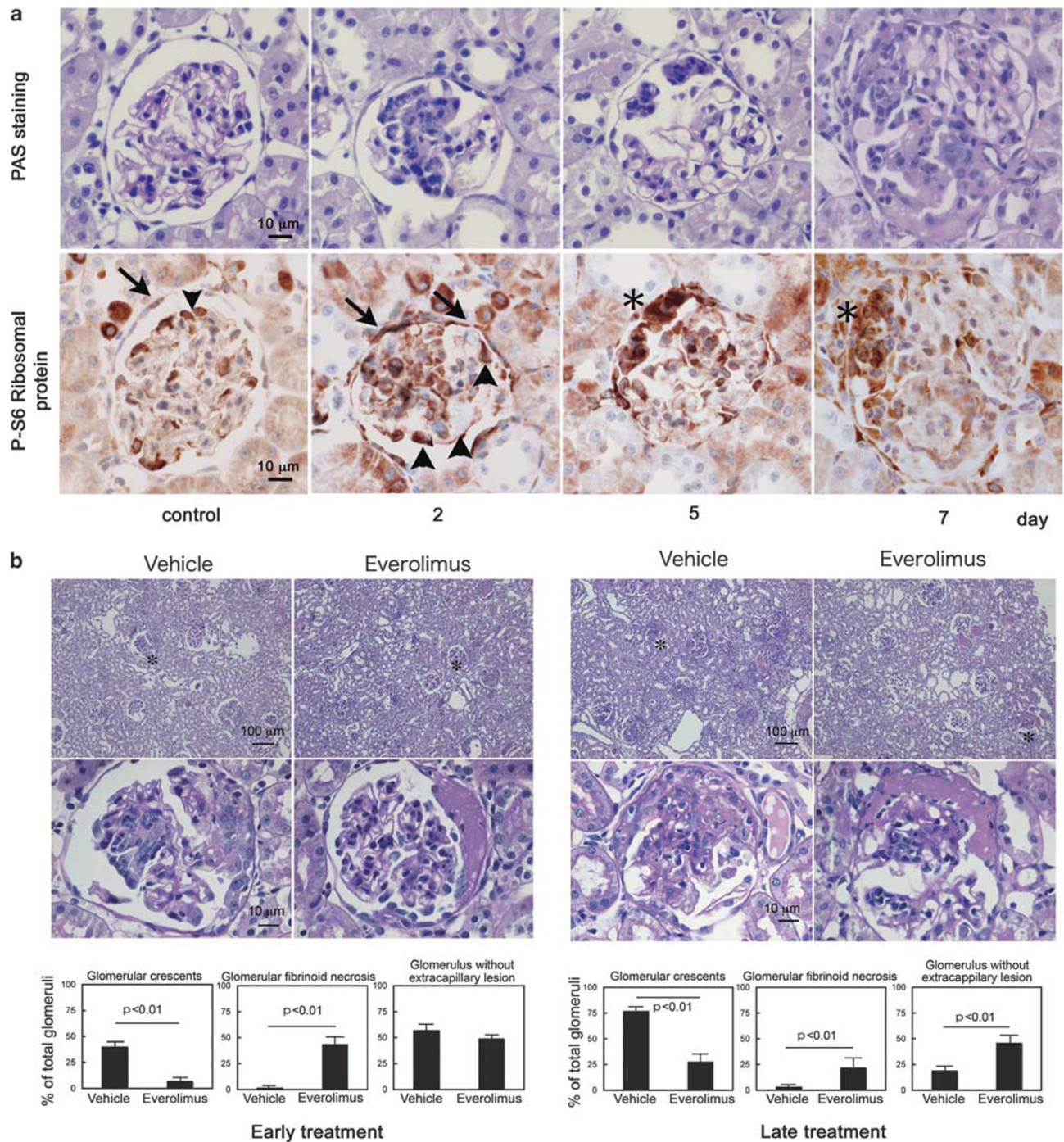


**Figure 3** Mammalian target of rapamycin complex 1 (mTORC1) activation in crescentic glomerulonephritis (CGN). (a) Immunohistochemistry of phosphorylated forms of S6 ribosomal protein (P-S6 ribosomal protein) and periodic acid-Schiff (PAS) staining by using serial sections. Arrow, arrowhead and asterisk indicate parietal epithelial cells (PECs), podocytes and cellular crescents, respectively. Scale bar = 10  $\mu$ m. (b) Effects of early and late treatment with everolimus on crescentic glomerulonephritis (CGN). CGN was induced in rats by injection of anti-glomerular basement membrane (GBM) antibody on day 0 and daily treatments with everolimus (2.5 mg/kg body weight) or vehicle solution were started either on day 0 (early treatment) or on day 7 (late treatment). Effects of early or late treatment on the glomerular morphology and histology showing cellular crescents and fibrinoid sclerosis. Lower panels were glomeruli enlarged from \* of upper panels. Histogram shows summary of renal injury analysis presented as ratio of glomerular cellular crescent, glomerular fibrinoid necrosis and glomeruli without extracapillary lesions.

using glomeruli isolated by the modified version of the magnetic beads method in which collagenase treatment was excluded from the procedure to preserve the integrity of the

Bowman's capsule. As shown in Figure 4b, whole glomeruli with intact Bowman's capsule could be isolated (arrow). Interestingly, this modified method also allowed us to isolate



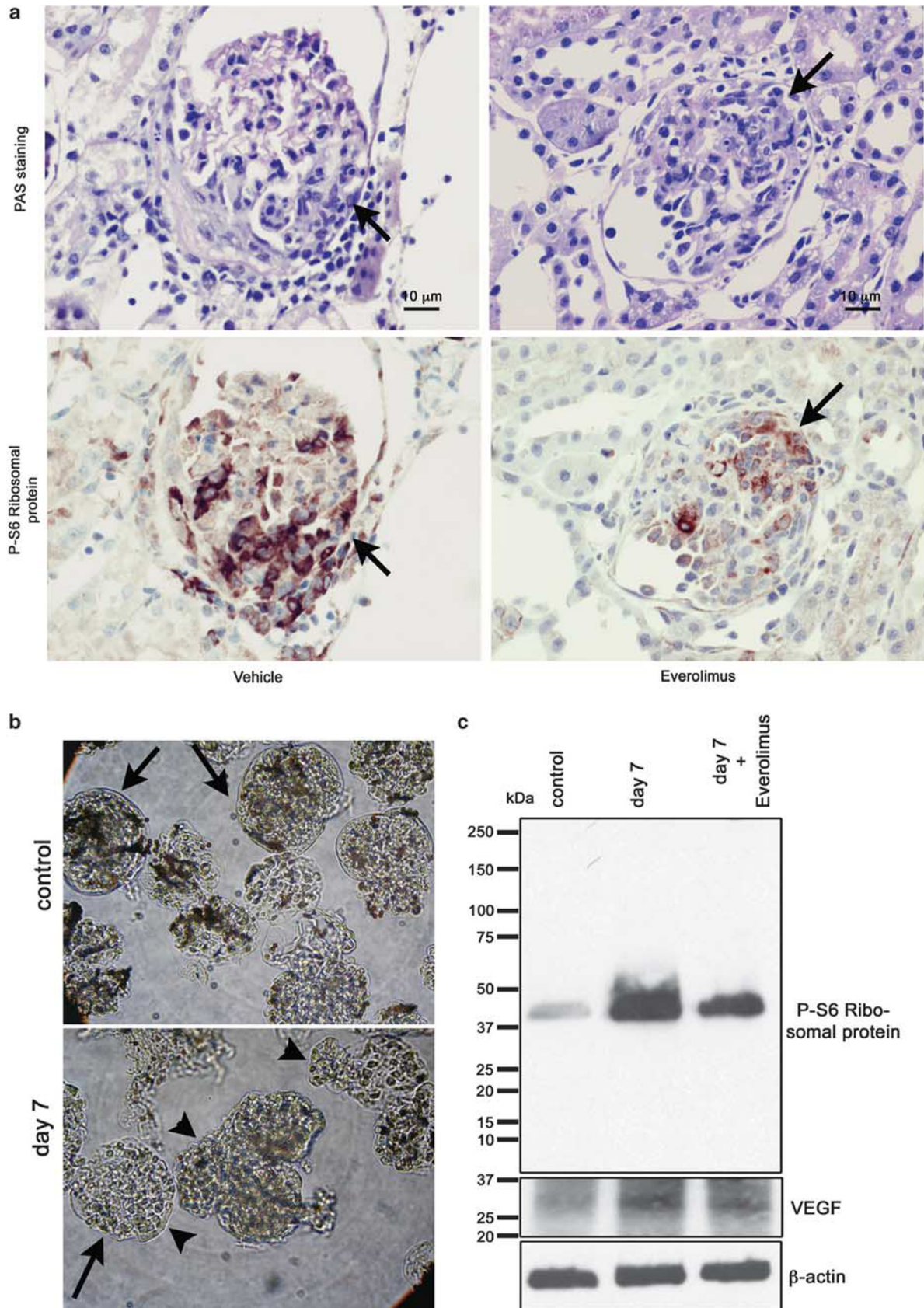


**Figure 4** For legend please see page 998.

crescentic glomeruli from rats on day 7 (Figure 4b, arrow-head). Western blot analysis of these samples revealed an apparent increase of p-S6RP of CGN glomeruli on day 7 (Figure 4c). When everolimus was administered, p-S6RP expression of CGN glomeruli was clearly abrogated (Figure 4c). These data strongly suggested a possible implication of mTORC1-mediated activation at an early stage of CGN. Unexpectedly, the outcome of everolimus in early treatment was worse than that of vehicle (Figure 3b). It is known that mTORC1 signaling stimulates angiogenesis and therefore mTOR inhibitors could have an inhibitory role in the angiogenesis system.<sup>43</sup> The same samples from the isolated glomeruli were subjected to western blot study with VEGF. Expression of VEGF was upregulated in day 7 glomeruli of CGN rats compared with that of control rat glomeruli

(Figure 4c). In contrast, this increase of VEGF expression was abrogated when everolimus was administered into CGN rats (Figure 4c), suggesting a protective role of VEGF interacted with mTORC1 in the integrity of diseased glomeruli of CGN.

Finally, we further verified the specific involvement of mTORC1 activation in the pathogenesis of crescent formation of CGN. Western blot analysis revealed that phospho-AKT1,<sup>38</sup> downstream of mTORC2, was also increased in the day 7 glomeruli of CGN compared with that of control glomeruli (Figure 5a). However, immunohistochemistry showed that the increased expression of phospho-AKT1 was distinctly revealed in the proliferated mesangial cells (arrow), not in cellular crescent lesions (asterisk) (Figure 5b), supporting the specific implication of mTORC1 activation in the pathogenesis of crescent formation.

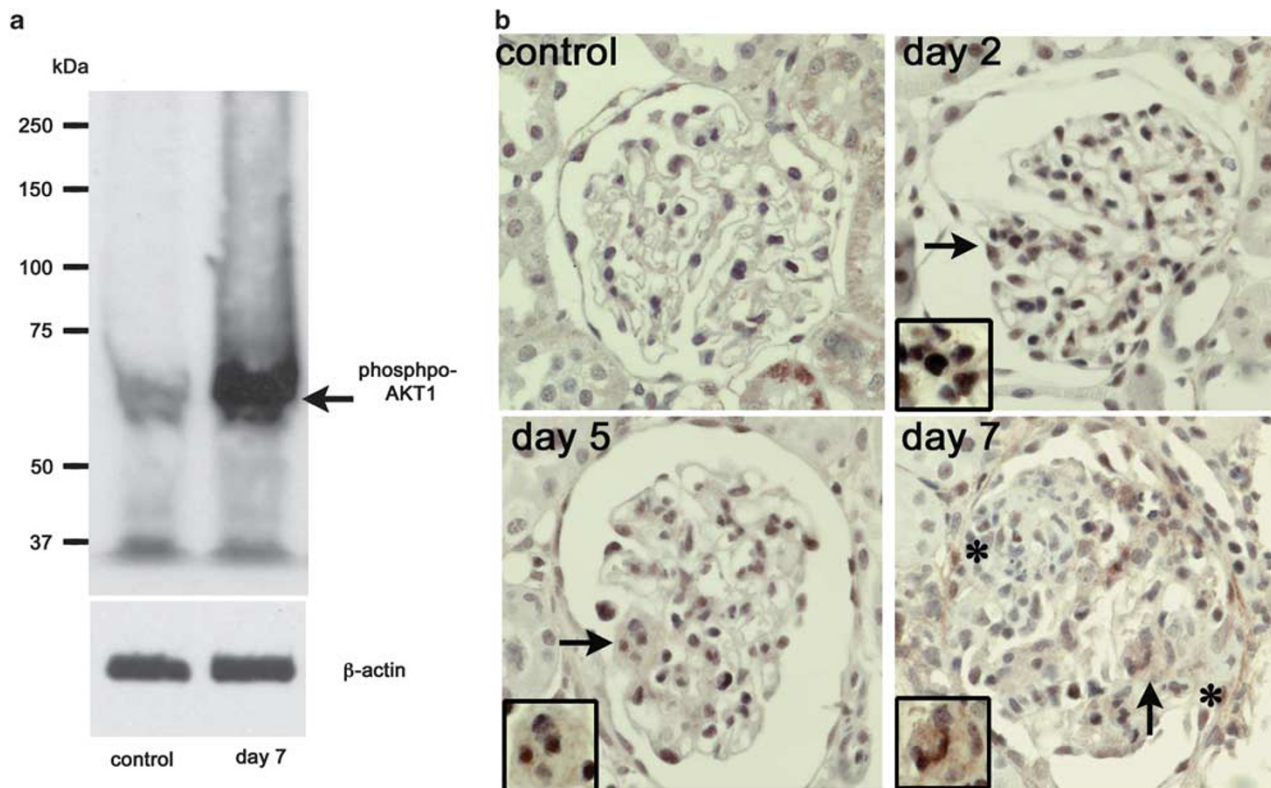


**Figure 5** Activation of mammalian target of rapamycin complex 2 (mTORC2) in crescentic glomerulonephritis (CGN) glomeruli. (a) Western blot analysis shows a marked increase of phospho-AKT1 in CGN glomeruli (day 7) compared with control glomeruli.  $\beta$ -Actin shows internal control of each sample. (b) Immunohistochemistry reveals that the main lesion of increased phospho-AKT1 is in the proliferative mesangial cells (arrow), not in the crescent lesion (asterisk), in CGN glomerulus of day 2, day 5 and day 7.

**Figure 4** Effect of everolimus on activation of S6 ribosomal protein in crescentic glomerulonephritis (CGN) glomerulus. (a) Immunohistochemistry and periodic acid-Schiff (PAS) staining examined by using serial sections revealed apparent reduction of phospho-S6 ribosomal protein in the crescent lesions (arrow) of everolimus-treated CGN. (b) Isolated glomeruli by using magnetic beads without collagenase treatment. Arrow indicates Bowman's capsule and arrowhead indicates crescents, respectively. (c) Western blot analysis by using protein samples from isolated glomeruli. Phospho-S6 ribosomal protein and vascular endothelial growth factor (VEGF) of the glomeruli from CGN (day 7) are strongly increased compared with that of control, whereas everolimus clearly abrogated upregulation of both proteins of CGN glomeruli.  $\beta$ -Actin shows internal control of each sample.

### Expression of LATs in Normal and Crescentic Glomeruli

We have previously shown podocyte-specific expression of LAT3 in both human and mouse glomerulus.<sup>38</sup> On the other hand, there has been no vigorous study showing the expression of LAT1 and LAT2 in the glomerulus. Therefore, we investigated the expression levels of LAT1, LAT2 and LAT3 in the isolated glomeruli and kidney sections. Western blot analysis revealed the presence of LAT1, LAT2 and LAT3 in the isolated glomerular extract of control rats, migrating as 42, 42 and 58 kDa protein bands, respectively (Figure 6a). Knowing that all three LATs were expressed in normal rat glomeruli, we next examined the cellular localization of these LATs in the kidney sections of control and CGN rats. As shown in Figure 6b, immunohistochemistry showed that LAT1 was faintly detected in the cytoplasm of PECs and podocytes of control rats. The immunostaining intensity of LAT1, however, was increased in the kidney sections of CGN rats on day 7, although its subcellular granular pattern in the cytoplasm remained unchanged (Figure 6b, day 7, inset). Positive staining of LAT1 in the capillary endothelial cells of blood-brain barrier<sup>30,31</sup> further confirmed the specificity of the anti-LAT1 antibody (Figure 6b, control, inset). A previous study showed a predominant expression of LAT2 at the basolateral membrane of proximal tubules.<sup>37</sup> Our immunohistochemistry confirmed the previous report and further revealed that LAT2 could also be found in the PECs and podocytes of normal (control) rat glomerulus (Figure 6b). However, similar to LAT1, the glomerular expression of LAT2 was faint and limited to the cytoplasm (Figure 6b, control). Interestingly, the relative expression of LAT2 in the glomeruli of CGN rats was significantly increased on day 7, especially in the cellular crescent lesions in which a plasma membrane distribution was also visible (Figure 6b, day 7, arrow, inset). In contrast to both LAT1 and LAT2, the glomerular expression of LAT3 in the control rats was limited to the podocyte plasma membrane, as we previously reported.<sup>38</sup> There was no apparent increase in the levels of LAT3 in the crescent lesions of CGN rats (Figure 6b, arrow, day 7). These findings suggested that, among the LATs studied here, only the expression of LAT2 was noticeably affected during the 7-day course of the study and, thus, LAT2 may exert some functional role in the activation of mTORC1 during the crescent formation.

A common molecular characteristic shared by LAT1 and LAT2 is that both form heterodimeric complex via disulfide bonds with 4F2hc that is required for the localization of LAT1 and LAT2 in the plasma membrane.<sup>27,37</sup> Therefore, we next examined the immunolocalization of LAT2 and its

ligand glycoprotein 4F2hc in the kidney sections of CGN rats. In the glomeruli of control rats, LAT2 was moderately expressed in the cytoplasm of PECs and podocytes, whereas 4F2hc was faintly detectable in these cells (Figure 7a). On day 2 after the insult, the intensity of LAT2 expression in the PECs and podocytes was increased and its subcellular localization partly shifted to the plasma membrane (Figure 7a). Although we did not find any change in the expression levels of 4F2hc in the PECs and podocytes on day 2, we could see some shift in its subcellular localization from cytoplasm to the plasma membrane (Figure 7a). When cellular crescents appeared on day 7, however, expression of both molecules in the plasma membrane of PECs and podocytes in the crescent drastically increased and its localization was clearly shifted to the plasma membrane (Figure 7a, day 7). Using RT-PCR on total RNA isolated from glomeruli of the same rats, we further confirmed the increase of LAT2 and its ligand 4F2hc at the mRNA level. As shown in Figure 7b, the relative mRNA levels of both LAT2 and 4F2hc in the glomeruli were significantly increased on day 2 and day 7, although their expression in the rest part of the kidney cortex after isolation of glomeruli remained relatively unchanged (Figure 7b).

### Activation of mTORC1 in Cells Expressing LAT2

As described earlier, BCAAs are known to be potent intracellular stimulators of mTORC1 activation.<sup>21–23,44</sup> Our current data, thus far, clearly pointed to an interrelationship between activation of mTORC1 pathway and upregulation of LAT2 in the glomeruli of rats at 2 days after the induction of CGN before histological signs of crescent formation. However, whether upregulation of LAT2 itself could lead mTORC1 activation was not clear because there has been very few data showing that existence of amino acid transporter on the plasma membrane itself could function as a direct entrance that activates mTORC1 cascade. To address this question, we next examined whether the presence and activity of LAT2 on the plasma membrane triggers activation of mTORC1. As there was no available cell line expressing endogenous LAT2 on the plasma membrane, we tested an amino acid starvation experiment by using the S2-hLAT2 cells, a cell line stably expressing recombinant human LAT2.<sup>42</sup> We first confirmed the expression and the plasma membrane localization of LAT2 in this cell line by western blot analysis and surface immunofluorescence staining, respectively. As shown in Figure 8a, western blot analysis of cellular extracts from S2-hLAT2 cell line clearly showed the presence of human LAT2 migrating as a 45-kDa protein. As expected, LAT2 could not be detected in the protein extracts of the wild-type

**Figure 6 (a and b)** Protein expression of L-type neutral amino acid transporter (LAT) isoforms in control and crescentic glomerulonephritis (CGN) kidney. **(a)** Western blot analysis of LAT isoforms in the samples of 50 µg protein from the isolated glomeruli (glo) and the rest of the kidney (cort) of the control rat kidney. β-Actin shows internal control of each sample. **(b)** Immunohistochemistry of LAT isoforms in the kidney of control and CGN on day 7. Inset in L-type neutral amino acid transporter (LAT)1 panel of control shows LAT1 expression in the capillary endothelial cells of the brain as a positive control. Insets in LAT1 and LAT2 of day 7 show enlargement from arrow. Arrowhead indicates plasma membrane localization of LAT2 in cellular crescent of day 7 glomerulus.



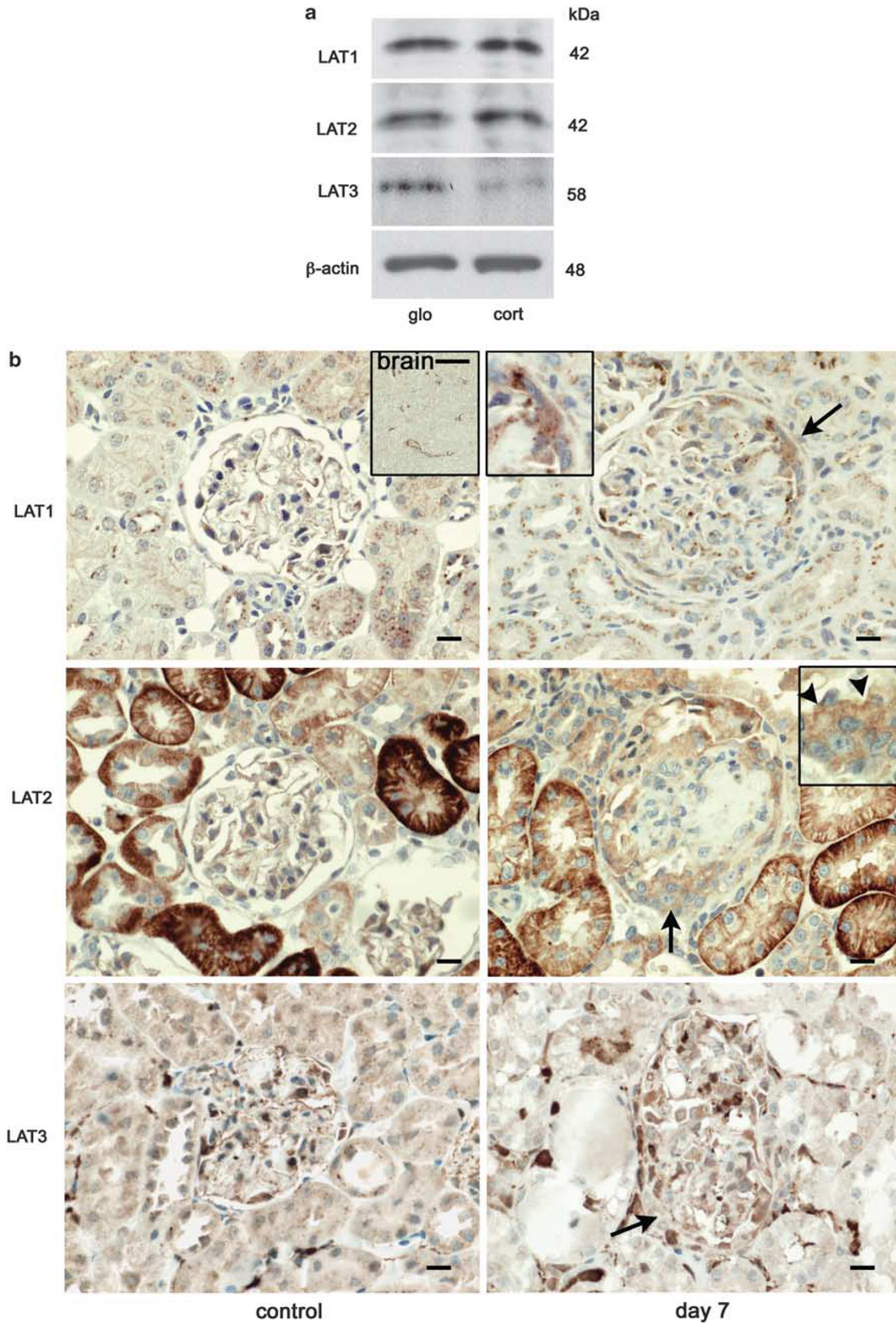


Figure 6 For legend please see page 999.



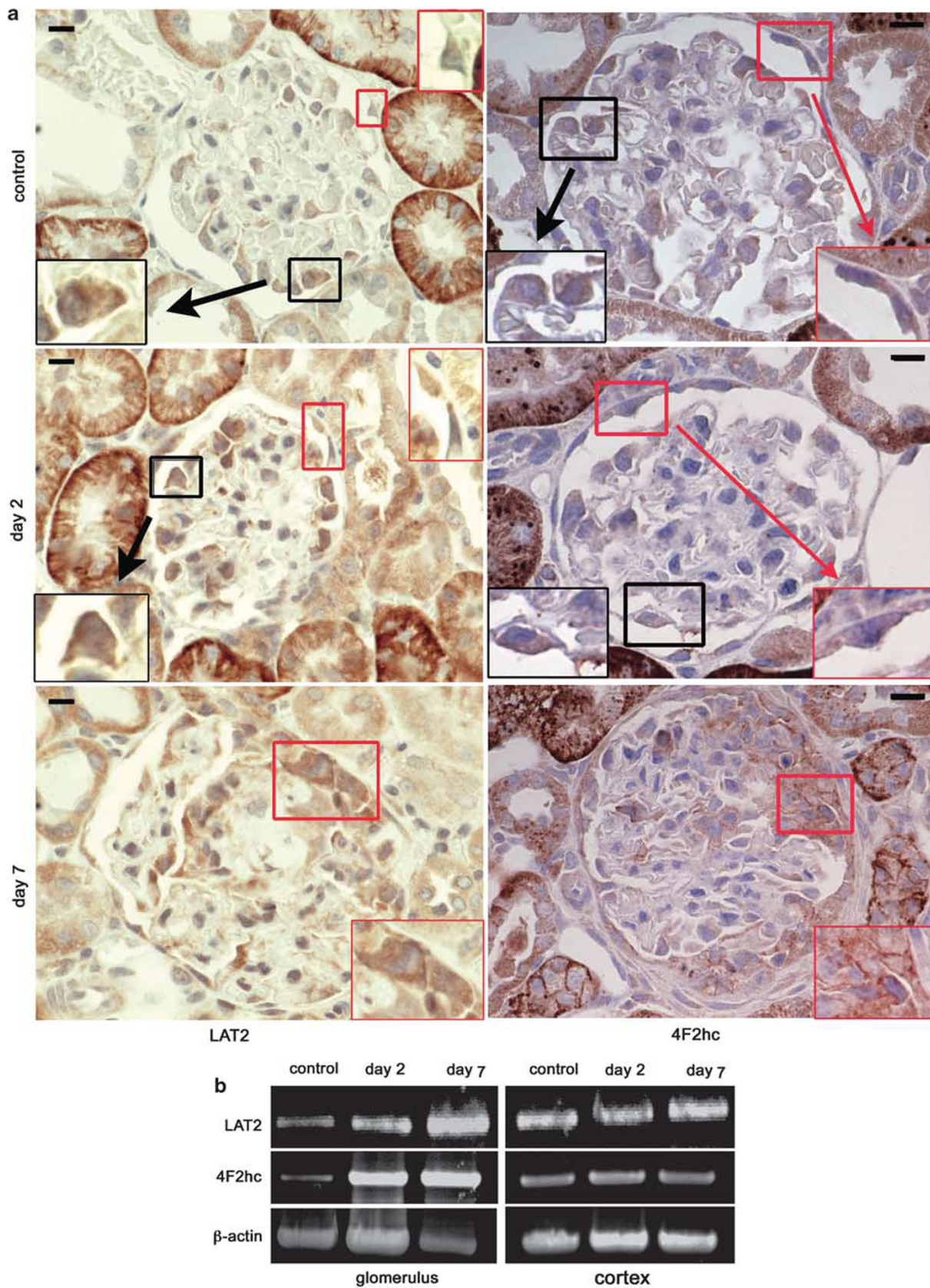


Figure 7 For legend please see page 1002.

S2 cell line (Figure 8a). Confocal microscopy of surface immunofluorescence-stained cells further confirmed the plasma membrane localization of LAT2 in the S2-hLAT2 cell line but not in the wild-type S2 cells (Figure 8b).

We next performed the mTORC1 assay by subjecting the S2-hLAT2 cells to amino acid starvation experiment. Cell lysates were subjected to western blot analysis to examine the activation of mTORC1 pathway by quantifying the degree of downstreams of mTORC1, phosphorylation of p70S6K and 4E-BP1 molecules. Figures 9a and b showed the time-dependent changes of activation with p70S6K and 4E-BP1 as a ratio of their phosphorylated forms over their non-phosphorylated forms in the absence or presence of the LAT2-inhibitor BCH. This analysis clearly showed that, in the absence of LAT2-inhibitor, activation of both proteins in the S2-hLAT2 cells started as early as 30 min and markedly increased by time up to 120 min (Figures 9a and b). However, this apparent increase in protein phosphorylation and activation was significantly abrogated in the presence of LAT-inhibitor, indicating that LAT2 is most likely to function as an upstream of mTORC1-mediated activation.

### Inhibitory Effect of LAT Inhibitor on Crescent Formation

Finally, to further verify a direct evidence of the role of LAT2 as one of initiators leading to crescent formation of CGN, we

examined the inhibitory effect of BCH in CGN rats. BCH is a reagent that specifically inhibits the activity of LAT1 and LAT2. However, on the basis of the data described above, LAT1 is not likely to function as an upstream of mTORC1 activation in CGN. Thus, BCH seems to inhibit only LAT2 function in CGN kidney. As depicted in Figure 10, treatment with BCH in CGN rats clearly reduced the ratio of cellular crescent on day 7 glomeruli when compared with glomeruli of rats injected by saline solution as control. Moreover, interestingly, BCH treatment did not increase the ratio of fibrinoid necrosis (Figure 10), which was different from the data that everolimus early treatment rather increased fibrinoid necrosis in the CGN glomeruli (Figure 3b).

### DISCUSSION

The mTOR is an evolutionarily conserved Ser/Thr protein kinase that forms a catalytic core of at least two functionally distinct signaling complexes, mTORC1 and mTORC2.<sup>45</sup> These complexes contain both unique and shared protein partners that collectively control many cellular processes in response to environmental stimuli such as growth factors and nutrients. Although mTORC2 is known to control actin cytoskeleton organization in a rapamycin-independent pathway, mTORC1 senses and integrates diverse extra- and intracellular signals to promote cell growth and proliferation

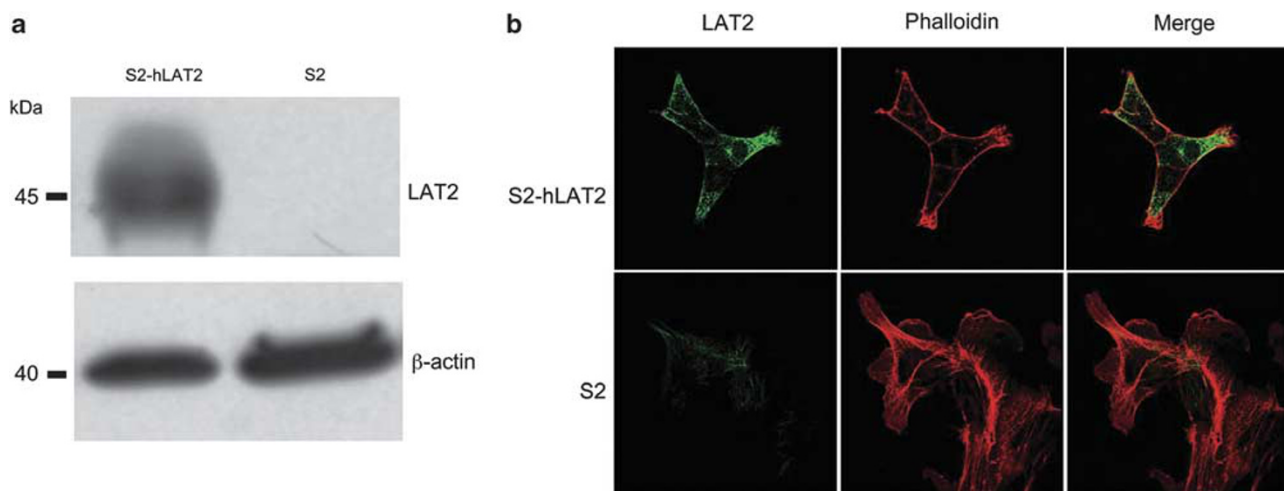


**Figure 8** (a and b) Expression and cellular localization of human L-type neutral amino acid transporter (LAT)2 in the transfected S2-hLAT2S2 cell line and S2 control cell line. (a) Western blot analysis shows positive expression of the human LAT2 in S2-hLAT2 cells migrating as a 45-kDa protein. The control cell (S2) shows no expression of LAT2.  $\beta$ -Actin as control shows the protein loading in each well. (b) Confocal microscopy of immunofluorescence-labeled cells shows plasma membrane localization of LAT2 in S2-hLAT2 cells and the lack of expression in the control cells. Phalloidin staining shows intracellular actin cytoskeleton.

**Figure 7** (a and b) Expression of L-type neutral amino acid transporter (LAT)2 and 4F2hc in the glomeruli of control and anti-glomerular basement membrane (GBM) glomerulonephritis rats. (a) Immunohistochemistry of LAT2 and 4F2hc in the glomerulus of control, day 2 and day 7 after injection of anti-GBM antibody. Larger insets show a higher magnification of the smaller insets. Scale bar = 10  $\mu$ m. (b) RT-PCR of mRNAs encoding LAT2 and 4F2hc from isolated glomeruli and the rest of the kidney of control, day 2 and day 7.  $\beta$ -Actin was used as an internal control.

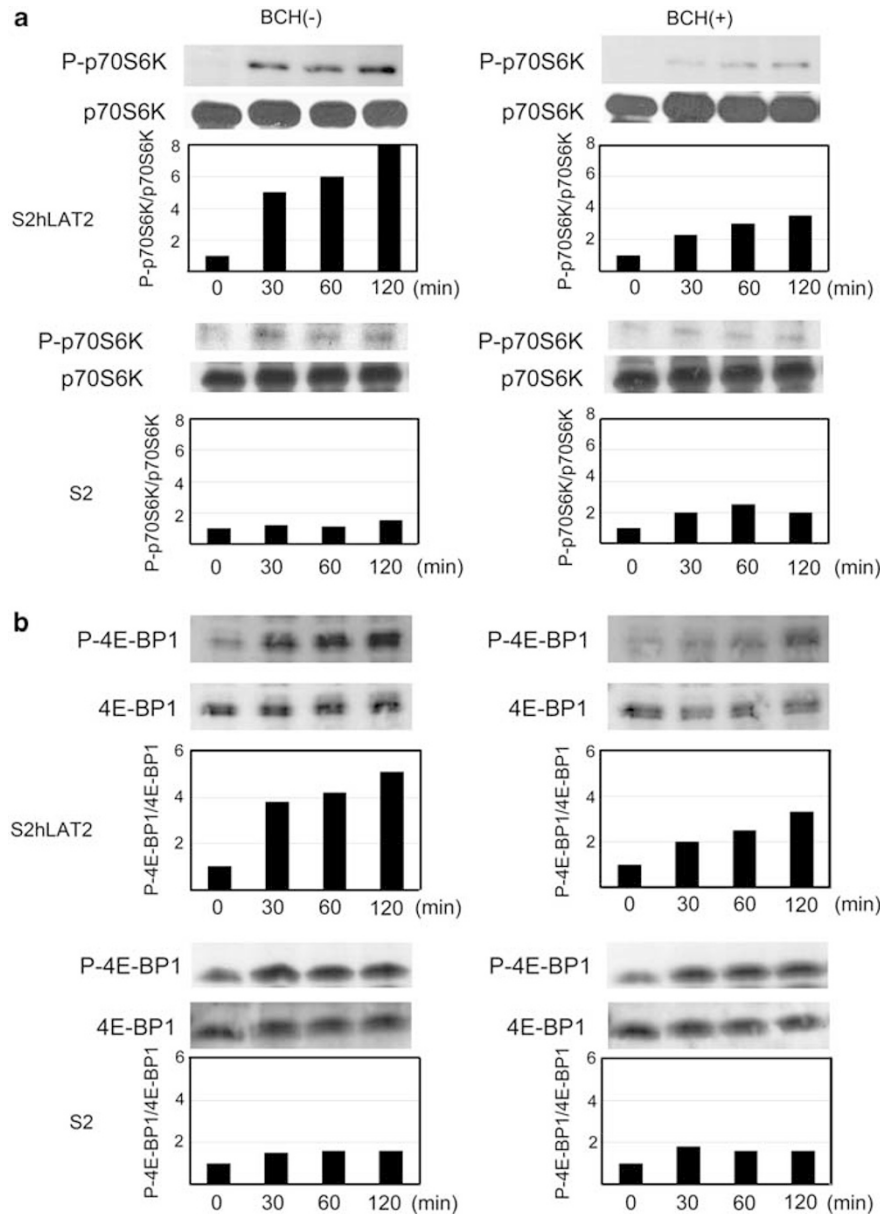


**Figure 9 (a and b)** Amino acid starvation assay shown by western blot analysis with the activation of mammalian target of rapamycin complex 1 (mTORC1) pathway, 70S6K and 4E-BP1, in the absence or presence of L-type neutral amino acid transporter (LAT)-specific inhibitor BCH. Histograms show the comparison for the level of activation of both molecules, expressed by the amount of phosphorylated form over total protein. **(a)** Activation of p70S6K occurred at 30 min after nutrition supply and was sustained for 120 min. BCH clearly abrogated p70S6K activation. **(b)** Activation of 4E-BP1 was determined as a similar pattern to p70S6K.

in a rapamycin-sensitive manner. Modulation of cellular growth and proliferation by mTORC1 is achieved via phosphorylation of downstream effectors: p70S6K, 4E-BP1 and S6-RP.<sup>46,47</sup> It is increasingly evident that elevation in the intracellular levels of BCAAs stimulates phosphorylation of these molecules, whereas deprivation of such amino acids promotes dephosphorylation of them.<sup>21,23,44</sup> However, mechanisms by which mTORC1 can sense changes in the levels of amino acids remain largely elusive.

The involvement of mTORC1 activation in the pathogenesis of several glomerular diseases has been reported, showing that

ischemia-reperfusion injury stimulates mTOR activity and inhibition of mTOR pathway by rapamycin delays renal recovery.<sup>48,49</sup> Several studies have also suggested that mTOR activation has a crucial role in the pathogenesis of kidney hypertrophy and increase of matrix proteins in the GBM in diabetic nephropathy.<sup>50,51</sup> However, to our knowledge, there has been only one report on the role of mTOR activation in anti-GBM nephritis showing that pretreatment of rapamycin protected glomerular injury through affecting T- and B-cell activation.<sup>52</sup> However, the typical glomerular change in their animal model was severe mesangial expansion and not CGN.



A major finding in the present study is that activation of mTORC1 pathway commenced in the glomerular PECs and podocytes before apparent crescent formation and increased in the crescent lesion itself of CGN (Figure 3a). Moreover, upregulation of LAT2 and its ligand 4F2hc also commenced in both glomerular epithelial cells before the crescent formation and further increased in the crescent lesions (Figures 6 and 7). These data suggest that coordination of upregulated LAT2 and 4F2hc and activation of mTORC1 signaling pathway in the glomerular epithelial cells may underlie a possible pathomechanism of crescent formation in CGN. Interestingly, we found that both LAT2 and 4F2hc exist even in the normal glomerular epithelial cells, but were localized in the cytoplasm. However, before crescent formation after glomerular injury, both LAT2 and 4F2hc of PECs and

podocytes were revealed in the plasma membrane. This suggests that LAT2 may not function as amino acid transport in the normal glomerular epithelial cells, but rather becomes immediately active once it relocated to the plasma membrane of PECs and podocytes even at the early stage of CGN after glomerular insult. Then a question arose as to what is a mechanism by which LAT2 and 4F2hc were upregulated and relocated and how mTORC1 was activated in the glomerular epithelial cells in CGN. Figure 11 shows our hypothesis for this question. It has been shown that interleukins-2 and -3 stimulate the surface expression of 4F2hc of mammalian cells.<sup>53,54</sup> and that the levels of LAT1 and 4F2hc are upregulated in the activated T-cells as compared with quiescent T-cells.<sup>55</sup> As 4F2hc is a key ligand glycoprotein required for the localization of LAT2 in the plasma membrane,<sup>27,37</sup> it is very likely that at first circulating cytokines and growth factors through ruptured GBM upregulated 4F2hc and LAT2 and subsequently stimulated the plasma membrane expression of 4F2hc (Figure 11, a). This 4F2hc expression in the plasma membrane appears to be crucial for LAT2 that can exist and function in the plasma membrane as an amino acid transporter (Figure 11, b).

Our amino acid starvation assay of cells expressing LAT2 further showed that the presence in the plasma membrane of LAT2 was essential for an increased phosphorylation of the downstream effectors of mTORC1 (p70S6K and 4E-BP1), whereas specific inhibition of LAT2 led to an inhibition of phosphorylation (Figure 9). This is also consistent with the recent finding demonstrating that the amino acid leucine can induce phosphorylation and activation of p70S6K in cortical neurons via activation of LATs.<sup>56</sup> Thus, it is most likely that

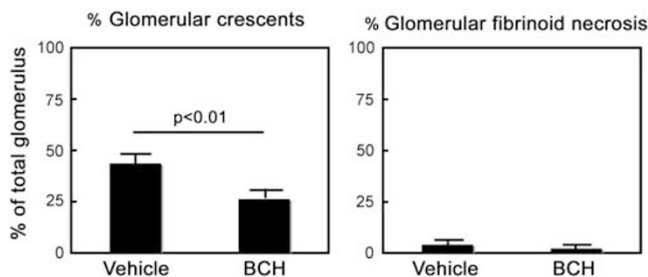


**Figure 10** Protective effect of BCH on the progression of CGN. BCH was administered at day 0 just after injection of anti-glomerular basement membrane (GBM) antibody. Histogram shows summary of renal injury analysis presented as ratio of cellular crescent and glomerular fibrinoid necrosis.

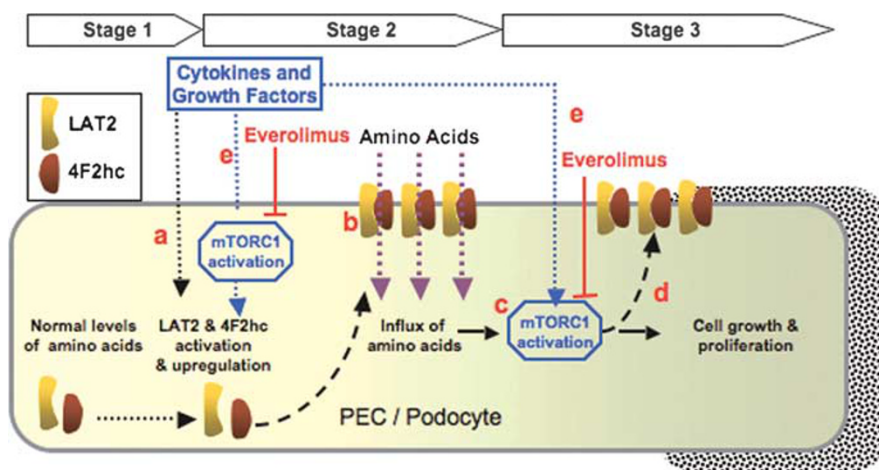


**Figure 11** Possible signaling pathway underlying pathogenesis of crescentic glomerulonephritis. In the normal glomerular parietal epithelial cells and podocytes (stage 1), L-type neutral amino acid transporter (LAT2) may not be involved in the normal amino acid homeostasis. In an early stage of disease (stage 2), cytokines and growth hormones act directly on mammalian target of rapamycin complex 1 (mTORC1) signaling pathway. Cytokines and growth hormones in addition to activated mTORC1 pathway upregulated LAT2 and its ligand 4F2hc. Subsequently, the complex of LAT2-4F2hc is relocated to the plasma membrane and increases the influx of amino acids (stage 2). This leads to the activation of mTORC1 signaling pathway, which results in cell hypertrophy, proliferation and crescent formation in the glomerulus. Treatment with mTORC1 inhibitor everolimus at a later stage can slow down the progression toward cellular lesions.

presence of LAT2–4F2hc in the plasma membrane of PECs and podocytes is crucial for induction of mTORC1 activation (Figure 11, c). Moreover, the fact that TOR controls the expression and trafficking of yeast nutrient transporters<sup>57</sup> strongly suggests that mTORC1 activation itself may further stimulate and maintain the expression and functional activation of LAT2–4F2hc complex in the plasma membrane in a paracrine manner (Figure 11, d).

mTORC1 is also induced by cytokines and growth factors, as well as amino acids.<sup>43,45</sup> This suggests a potential cascade by such molecules, directly inducing mTORC1 during the progress of CGN (Figure 11, e). Increased LAT2 activity and these stimuli from cytokines and growth factors may consequently result in activation of mTORC1 pathway at stage 3, which subsequently leads to cell growth and proliferation and crescent formation. At this stage 3, treatment with everolimus can prevent cellular proliferation and maintain intact glomeruli. But, we found that early treatment with everolimus led to an increase in the cellular necrosis of the glomerular PECs. Although this result may seem paradoxical, it could suggest that premature treatment with everolimus might thoroughly disrupt protein synthesis system through affecting mTORC1 pathway at the stage 2 (Figure 11, stage 2, e). This pathway must be essentially required for a flexible system of protein synthesis opposing insult in glomerular PECs of the early stage of CGN. Therefore, it is also speculated that hypertrophy and proliferation of glomerular PECs may be one of the protective phenomena to overcome insult. Interestingly, LAT-specific inhibitor BCH protected the progress of cellular crescents and further did not increase fibrinoid necrosis of CGN unlike everolimus treatment (Figure 11). BCH is not likely to inhibit protein synthesis system itself. Although there has been no study with regard to the nutritional transport system in glomerular epithelial cells except our previous<sup>38</sup> and present data, it could suggest that many complicated transport systems of nutrition compensated the lack of LAT2 function in PECs of CGN. More studies are required to investigate the dose- and time-dependent effects of everolimus as a possible candidate of therapeutic agents for CGN.

Supplementary Information accompanies the paper on the Laboratory Investigation website (<http://www.laboratoryinvestigation.org>)

#### ACKNOWLEDGEMENTS

This work was supported by The Ministry of Education, Culture, Sport, Science and Technology of Japan, KAKENHI (C18590901). We thank Ms Y Kimura for the excellent technical assistance.

#### DISCLOSURE/CONFLICT OF INTEREST

The authors declare no conflict of interest.

1. Wiggins RC HL, Legault DJ. Glomerular inflammation and crescent formation. In: Neilson EG, Couser WG (eds). *Immunologic Renal Diseases*. Lippincott-Raven: Philadelphia, 1997, pp 669–682.

2. Magil AB. Histogenesis of glomerular crescents. Immunohistochemical demonstration of cytokeratin in crescent cells. *Am J Pathol* 1985;120: 222–229.
3. Morita T, Suzuki Y, Churg J. Structure and development of the glomerular crescent. *Am J Pathol* 1973;72:349–368.
4. Min KW, Gyorkey F, Gyorkey P, *et al*. The morphogenesis of glomerular crescents in rapidly progressive glomerulonephritis. *Kidney Int* 1974;5:47–56.
5. Ophascharoensuk V, Pippin JW, Gordon KL, *et al*. Role of intrinsic renal cells versus infiltrating cells in glomerular crescent formation. *Kidney Int* 1998;54:416–425.
6. Guettier C, Nochy D, Jacquot C, *et al*. Immunohistochemical demonstration of parietal epithelial cells and macrophages in human proliferative extra-capillary lesions. *Virchows Archiv* 1986;409: 739–748.
7. Le Hir M, Keller C, Eschmann V, *et al*. Podocyte bridges between the tuft and Bowman's capsule: an early event in experimental crescentic glomerulonephritis. *J Am Soc Nephrol* 2001;12: 2060–2071.
8. Moeller MJ, Soofi A, Hartmann I, *et al*. Podocytes populate cellular crescents in a murine model of inflammatory glomerulonephritis. *J Am Soc Nephrol* 2004;15:61–67.
9. Smeets B, Uhlig S, Fuss A, *et al*. Tracing the origin of glomerular extracapillary lesion from parietal epithelial cells. *J Am Soc Nephrol* 2009;20:2604–2615.
10. Abboud HE. Growth factors in glomerulonephritis. *Kidney Int* 1993;43:252–267.
11. Kitching AR, Turner AL, Wilson GR, *et al*. IL-12p40 and IL-18 in crescentic glomerulonephritis: IL-12p40 is the key Th1-defining cytokine chain, whereas IL-18 promotes local inflammation and leukocyte recruitment. *J Am Soc Nephrol* 2005;16:2023–2033.
12. Lloyd CM, Minto AW, Dorf ME, *et al*. RANTES and monocyte chemoattractant protein-1 (MCP-1) play an important role in the inflammatory phase of crescentic nephritis, but only MCP-1 is involved in crescent formation and interstitial fibrosis. *J Exp Med* 1997;185: 1371–1380.
13. Song CY, Kim BC, Hong HK, *et al*. TGF-beta type II receptor deficiency prevents renal injury via decrease in ERK activity in crescentic glomerulonephritis. *Kidney Int* 2007;71:882–888.
14. Ono K, Han J. The p38 signal transduction pathway: activation and function. *Cell Signal* 2000;12:1–13.
15. Deng T, Karin M. c-Fos transcriptional activity stimulated by H-Ras-activated protein kinase distinct from JNK and ERK. *Nature* 1994;371:171–175.
16. Lee JC, Laydon JT, McDonnell PC, *et al*. A protein kinase involved in the regulation of inflammatory cytokine biosynthesis. *Nature* 1994;372:739–746.
17. Bokemeyer D, Guglielmi KE, McGinty A, *et al*. Activation of extracellular signal-regulated kinase in proliferative glomerulonephritis in rats. *J Clin Invest* 1997;100:582–588.
18. Polzer K, Soleiman A, Baum W, *et al*. Selective p38MAPK isoform expression and activation in antineutrophil cytoplasmic antibody-associated crescentic glomerulonephritis: role of p38MAPK $\alpha$ . *Ann Rheum Dis* 2008;67:602–608.
19. Dann SG, Thomas G. The amino acid sensitive TOR pathway from yeast to mammals. *FEBS Lett* 2006;580:2821–2829.
20. Yang Q, Guan KL. Expanding mTOR signaling. *Cell Res* 2007;17: 666–681.
21. Wang X, Campbell LE, Miller CM, *et al*. Amino acid availability regulates p70 S6 kinase and multiple translation factors. *Biochem J* 1998;334:261–267.
22. Proud CG. mTOR-mediated regulation of translation factors by amino acids. *Biochem Biophys Res Commun* 2004;313:429–436.
23. Kim E. Mechanisms of amino acid sensing in mTOR signaling pathway. *Nutr Res Pract* 2009;3:64–71.
24. Fox HL, Pham PT, Kimball SR, *et al*. Amino acid effects on translational repressor 4E-BP1 are mediated primarily by L-leucine in isolated adipocytes. *Am J Physiol* 1998;275:C1232–C1238.
25. Christensen HN. Role of amino acid transport and countertransport in nutrition and metabolism. *Physiol Rev* 1990;70:43–77.
26. Palacin M, Estevez R, Bertran J, *et al*. Molecular biology of mammalian plasma membrane amino acid transporters. *Physiol Rev* 1998;78: 969–1054.

27. Kanai Y, Segawa H, Miyamoto K, *et al*. Expression cloning and characterization of a transporter for large neutral amino acids activated by the heavy chain of 4F2 antigen (CD98). *J Biol Chem* 1998;273:23629–23632.
28. Yanagida O, Kanai Y, Chairoungdua A, *et al*. Human L-type amino acid transporter 1 (LAT1): characterization of function and expression in tumor cell lines. *Biochim Biophys Acta* 2001;1514:291–302.
29. Nakanishi K, Matsuo H, Kanai Y, *et al*. LAT1 expression in normal lung and in atypical adenomatous hyperplasia and adenocarcinoma of the lung. *Virchows Arch* 2006;448:142–150.
30. Matsuo H, Tsukada S, Nakata T, *et al*. Expression of a system L neutral amino acid transporter at the blood-brain barrier. *Neuroreport* 2000;11:3507–3511.
31. Kageyama T, Nakamura M, Matsuo A, *et al*. The 4F2hc/LAT1 complex transports L-DOPA across the blood-brain barrier. *Brain Res* 2000;879:115–121.
32. Ritchie JW, Taylor PM. Role of the system L permease LAT1 in amino acid and iodothyronine transport in placenta. *Biochem J* 2001;356:719–725.
33. Park SY, Kim JK, Kim IJ, *et al*. Reabsorption of neutral amino acids mediated by amino acid transporter LAT2 and TAT1 in the basolateral membrane of proximal tubule. *Arch Pharm Res* 2005;28:421–432.
34. Dave MH, Schulz N, Zecevic M, *et al*. Expression of heteromeric amino acid transporters along the murine intestine. *J Physiol* 2004;558:597–610.
35. Pineda M, Fernandez E, Torrents D, *et al*. Identification of a membrane protein, LAT-2, that co-expresses with 4F2 heavy chain, an L-type amino acid transport activity with broad specificity for small and large zwitterionic amino acids. *J Biol Chem* 1999;274:19738–19744.
36. Segawa H, Fukasawa Y, Miyamoto K, *et al*. Identification and functional characterization of a Na<sup>+</sup>-independent neutral amino acid transporter with broad substrate selectivity. *J Biol Chem* 1999;274:19745–19751.
37. Rossier G, Meier C, Bauch C, *et al*. LAT2, a new basolateral 4F2hc/CD98-associated amino acid transporter of kidney and intestine. *J Biol Chem* 1999;274:34948–34954.
38. Sekine Y, Nishibori Y, Akimoto Y, *et al*. Amino acid transporter LAT3 is required for podocyte development and function. *J Am Soc Nephrol* 2009;20:1586–1596.
39. Bodoy S, Martin L, Zorzano A, *et al*. Identification of LAT4, a novel amino acid transporter with system L activity. *J Biol Chem* 2005;280:12002–12011.
40. Kohda T, Okada S, Hayashi A, *et al*. High nephritogenicity of monoclonal antibodies belonging to IgG2a and IgG2b subclasses in rat anti-GBM nephritis. *Kidney Int* 2004;66:177–186.
41. Treberg JR, Clow KA, Greene KA, *et al*. Systemic activation of glutamate dehydrogenase: implications for the hyperinsulinism/hyperammonemia syndrome. *Am J Physiol Endocrinol Metab* 2010;298:E1219–E1225.
42. Morimoto E, Kanai Y, Kim do K, *et al*. Establishment and characterization of mammalian cell lines stably expressing human L-type amino acid transporters. *J Pharmacol Sci* 2008;108:505–516.
43. Seeliger H, Guba M, Kleespies A, *et al*. Role of mTOR in solid tumor systems: a therapeutic target against primary tumor growth, metastases, and angiogenesis. *Cancer Metastasis Rev* 2007;26: 611–621.
44. Fox HL, Kimball SR, Jefferson LS, *et al*. Amino acids stimulate phosphorylation of p70S6k and organization of rat adipocytes into multicellular clusters. *Am J Physiol* 1998;274:C206–C213.
45. Foster KG, Fingar DC. mTOR: conducting the cellular signaling symphony. *J Biol Chem* 2010;285:14071–14077.
46. Fingar DC, Richardson CJ, Tee AR, *et al*. mTOR controls cell cycle progression through its cell growth effectors S6K1 and 4E-BP1/eukaryotic translation initiation factor 4E. *Mol Cell Biol* 2004;24: 200–216.
47. Hay N, Sonenberg N. Upstream and downstream of mTOR. *Genes Dev* 2004;18:1926–1945.
48. Lieberthal W, Levine JS. The role of the mammalian target of rapamycin (mTOR) in renal disease. *J Am Soc Nephrol* 2009;20:2493–2502.
49. Lieberthal W, Fuhro R, Andry CC, *et al*. Rapamycin impairs recovery from acute renal failure: role of cell-cycle arrest and apoptosis of tubular cells. *Am J Physiol Renal Physiol* 2001;281:F693–F706.
50. Mariappan MM, Feliers D, Mummidi S, *et al*. High glucose, high insulin, and their combination rapidly induce laminin-beta1 synthesis by regulation of mRNA translation in renal epithelial cells. *Diabetes* 2007;56:476–485.
51. Chen JK, Chen J, Neilson EG, *et al*. Role of mammalian target of rapamycin signaling in compensatory renal hypertrophy. *J Am Soc Nephrol* 2005;16:1384–1391.
52. Hochegger K, Jansky GL, Soleiman A, *et al*. Differential effects of rapamycin in anti-GBM glomerulonephritis. *J Am Soc Nephrol* 2008;19:1520–1529.
53. Cornish GH, Sinclair LV, Cantrell DA. Differential regulation of T-cell growth by IL-2 and IL-15. *Blood* 2006;108:600–608.
54. Edinger AL, Thompson CB. Akt maintains cell size and survival by increasing mTOR-dependent nutrient uptake. *Mol Biol Cell* 2002;13:2276–2288.
55. Nii T, Segawa H, Taketani Y, *et al*. Molecular events involved in up-regulating human Na<sup>+</sup>-independent neutral amino acid transporter LAT1 during T-cell activation. *Biochem J* 2001;358:693–704.
56. Ishizuka Y, Kakiya N, Nawa H, *et al*. Leucine induces phosphorylation and activation of p70S6K in cortical neurons via the system L amino acid transporter. *J Neurochem* 2008;106:934–942.
57. Edinger AL. Controlling cell growth and survival through regulated nutrient transporter expression. *Biochem J* 2007;406:1–12.